AIP | Physics of Plasmas
#1 JOURNAL IN 2014 GOOGLE SCHOLAR METRICS FOR THE PLASMA & FUSION CATEGORY

Kinetic model of force-free current sheets with non-uniform temperature

D. Y. Kolotkov, I. Y. Vasko, and V. M. Nakariakov

Citation: Physics of Plasmas **22**, 112902 (2015); doi: 10.1063/1.4935488
View online: http://dx.doi.org/10.1063/1.4935488
View Table of Contents: http://scitation.aip.org/content/aip/journal/pop/22/11?ver=pdfcov
Published by the AIP Publishing

Kinetic model of force-free current sheets with non-uniform temperature

D. Y. Kolotkov,[1] I. Y. Vasko,[2] and V. M. Nakariakov[1]
[1]*Centre for Fusion, Space and Astrophysics, Physics Department, University of Warwick, Coventry, United Kingdom*
[2]*Space Research Institute, RAS, Moscow, Russia*

(Received 25 August 2015; accepted 27 October 2015; published online 11 November 2015)

The kinetic model of a one-dimensional force-free current sheet (CS) developed recently by Harrison and Neukirch [Phys. Rev. Lett. **102**(13), 135003 (2009)] predicts uniform distributions of the plasma temperature and density across the CS. However, in realistic physical systems, inhomogeneities of these plasma parameters may arise quite naturally due to the boundary conditions or local plasma heating. Moreover, as the CS spatial scale becomes larger than the characteristic kinetic scales (the regime often referred to as the MHD limit), it should be possible to set arbitrary density and temperature profiles. Thus, an advanced model has to allow for inhomogeneities of the macroscopic plasma parameters across the CS, to be consistent with the MHD limit. In this paper, we generalise the kinetic model of a force-free current sheet, taking into account the inhomogeneity of the density and temperature across the CS. In the developed model, the density may either be enhanced or depleted in the CS central region. The temperature profile is prescribed by the density profile, keeping the plasma pressure uniform across the CS. All macroscopic parameters, as well as the distribution functions for the protons and electrons, are determined analytically. Applications of the developed model to current sheets observed in space plasmas are discussed. © *2015 AIP Publishing LLC*. [http://dx.doi.org/10.1063/1.4935488]

I. INTRODUCTION

Current sheets (CSs) play a central role in the initiation of active phenomena in space, astrophysical, and laboratory plasmas.[39,49] In particular, CSs are believed to appear in the solar atmosphere,[35,37] solar wind,[20] planetary magnetospheres,[25,36] and in pulsar winds.[6] Magnetic reconnection occurring within CSs results in the transformation of the magnetic field energy into the kinetic energy of the plasma and accelerated non-thermal charged particles, and hence the kinetic bulk energy.[45,53] In addition, CSs act as effective waveguides for MHD waves[16,17,29,43] that could be responsible for solar coronal heating.[13] In turn, remote observations of the MHD waves guided by solar coronal CSs allow for diagnostics of properties of these CSs.[14,26,30,32]

The study of CS instabilities and properties of guided MHD waves requires the development of equilibrium CS models. Since space and astrophysical plasmas are often considered to be collisionless, the development of the CS models should be based on the set of Vlasov–Maxwell equations. More specifically, the widely used Harris model[22] presents a 1D kinetic CS with the magnetic field $\mathbf{B} = B_0 \tanh(z/L)\mathbf{e}_x$ (where B_0 is the magnetic field strength, and L is the CS thickness). In the Harris model, the variation of the magnetic pressure across the CS is compensated by the plasma pressure gradient. However, observations in the near Earth space have evidently required development of generalised Harris models that would take into account several plasma populations,[51,54] power-law energy distribution functions of charged particles,[18] a non-zero guiding magnetic field $B_y(z)$,[34,38] and a possible bifurcation (or splitting) of the current density profile.[9,19,50] These models have also been generalised for relativistic plasmas typical for pulsar winds.[5,28] CSs formed in planetary magnetotails often include a finite B_z component (directed across the current sheet plane, i.e., the magnetic reversal geometry) due to the planetary dipolar magnetic field. In 1D models including a finite B_z (see Refs. 41, 42, and 55), the tangential magnetic field stresses (along the x and y axes) are balanced by the non-diagonal elements of the pressure tensor. In contrast, in 2D generalisations of the Harris model, these stresses are balanced by the gradients of the isotropic gas pressure tensor.[7,10,11,27,47,52]

Force-free CSs constitute an important class of magnetoplasma structures formed particularly in low-β plasmas. Moreover, force-free CSs are the states of minimum energy for a closed magnetoplasma system with a fixed helicity.[8] In force-free CSs, the current density is predominantly field-aligned. Force-free CSs are thought to be typical for pulsar wind plasmas[21,31] and may also be formed in the solar corona.[37] In addition, force-free CSs are quite typical for the Jupiter magentotail[4] and sometimes are observed in the Earth's magnetotail.[3,46] Similar force-free CSs are formed in laboratory plasmas.[15]

The first kinetic model of a 1D force-free CS with the magnetic field $\mathbf{B} = B_0\tanh(z/L)\mathbf{e}_x + B_0\cosh^{-1}(z/L)\mathbf{e}_y$ was recently developed (see Refs. 23 and 33). In that model, the plasma pressure and the magnetic pressure $(B_x^2 + B_y^2)/8\pi$ are uniform across CS. In contrast to the models described above, in this case, the force balance is provided by the non-zero value of the shear magnetic field B_y instead of the plasma pressure gradient. Subsequently, this model has been generalised for non-Maxwellian distribution functions of charged particles[48] and relativistic plasmas.[44] Kinetic models of a force-free CS with a periodic transverse structure have also recently been developed.[1] Similar to the Harris model,

in Ref. 23, the CS thickness depends on the parameters of charged particles distribution functions and may be larger than the characteristic kinetic scales.

The class of force-free models suggested in Refs. 23 and 33 has one significant drawback. In these models, the plasma temperature and density distributions are uniform across the CS. However, in the case, when the CS spatial scale is much larger than the characteristic ion gyroradius (one can refer to this regime as an MHD limit, although the plasma can be collisionless), it should be possible to set arbitrary temperature and density profiles across the CS, keeping the uniform pressure to ensure the total pressure balance in the transverse direction. In a realistic physical system (e.g., in the solar atmosphere), the density and temperature distributions across the CS are prescribed by the boundary conditions at some surface (crossed by all field lines) and local heating mechanisms (e.g., the Ohmic heating that is localised in the region of the strongest electric current density). Thus, physical reasoning suggests that models developed in Refs. 23 and 33 set highly restrictive conditions on the density and temperature distributions. In the present paper, we generalise that model, incorporating inhomogeneous distributions of the plasma temperature and density in the direction across the CS.

II. ANALYSIS

It was shown (see, e.g., Refs. 24, 39, and 40) that for 1D CSs with the magnetic field $\mathbf{B} = B_x(z)\,\mathbf{e}_x + B_y(z)\,\mathbf{e}_y$ where the z-axis is directed across the CS, the set of Vlasov–Maxwell equations can be reduced to Ampere's law in the following form:

$$\frac{d^2A_x}{dz^2} = -4\pi\frac{\partial P_{zz}}{\partial A_x}, \tag{1}$$

$$\frac{d^2A_y}{dz^2} = -4\pi\frac{\partial P_{zz}}{\partial A_y}, \tag{2}$$

where A_x and A_y are the components of the magnetic field vector potential ($B_x = -dA_y/dz$ and $B_y = dA_x/dz$), and P_{zz} is the zz-component of the plasma pressure tensor. The latter is given by

$$P_{zz}(A_x, A_y, \phi) = \sum_{s=i,e}\int m_s v_z^2 f_s(\mathbf{v}, \mathbf{r})d^3\mathbf{v}, \tag{3}$$

where the indices $s = i, e$ are used for the plasma species designation (we consider an electron-ion plasma), ϕ is the scalar potential corresponding to the electric field $E_z = -d\phi/dz$ arising due to the electron–ion decoupling, m_s denotes the particle masses, and $f_s(\mathbf{v}, \mathbf{r})$ are the particles' distribution functions that satisfy the Vlasov equation.

The Vlasov equation can be solved by choosing the distribution function as an arbitrary function of the particles' integrals of motion. In the chosen 1D configuration, there are three integrals of motion: the total energy $H_s = m_s\mathbf{v}^2/2 + q_s\phi$ and two generalised momenta $p_{xs} = m_s v_x + q_s A_x$ and $p_{ys} = m_s v_y + q_s A_y$ (q_s is a particle charge, $q_i = -q_e \equiv e$), so that the Vlasov equation is solved by assuming $f_s(\mathbf{v}, \mathbf{r}) = f_s(H_s, p_{xs}, p_{ys})$. We consider CSs with the transverse scale exceeding the Debye length so that the plasma is assumed to be quasi-neutral. The quasi-neutrality condition can be written as $\partial P_{zz}/\partial\phi = 0$ (see Refs. 39 and 40). This condition allows one to determine the distribution of the electrostatic potential $\phi = \phi(A_x, A_y)$.

The standard procedure for developing a kinetic CS model consists of the choice of the particles' distribution functions and the analysis of Eqs. (1) and (2). An alternative, inverse approach is to set *a priori* a magnetic field configuration and determine the corresponding distribution functions.[12] The latter approach was chosen in Ref. 23 to develop the model of a 1D force-free CS with homogenous transverse profiles for density and temperature. We note that in the inverse approach[12] the distribution functions are not determined uniquely. In the present paper, we generalise the force-free CS model, including transverse inhomogeneities of the plasma parameters, by an appropriate choice of the particle distribution functions.

The magnetic field of a force-free Harris sheet has the following non-zero components:

$$B_x = B_0\tanh(z/L), \tag{4}$$

$$B_y = B_0\cosh^{-1}(z/L), \tag{5}$$

where the constants B_0 and L are the magnetic field amplitude and the CS characteristic scale length, respectively. The current densities corresponding to this magnetic field are $j_x = cB_0/(4\pi L)\tanh(z/L)/\cosh(z/L)$ and $j_y = cB_0/(4\pi L)\cosh^{-2}(z/L)$. The magnetic field components $B_x(z)$, $B_y(z)$ and the corresponding current densities are shown in Fig. 1. The vector potential corresponding to the force-free CS given by (4) and (5) has two components

$$A_x = 2B_0L\arctan(\exp(z/L)), \tag{6}$$

$$A_y = -B_0L\ln(\cosh(z/L)). \tag{7}$$

According to Harrison and Neukirch,[23] Eqs. (1) and (2) have the following solution $P_{zz}(A_x, A_y)$ in the class of additive functions, i.e., $P_{zz}(A_x, A_y) = P_1(A_x) + P_2(A_y)$:

$$P_{zz} = \frac{B_0^2}{8\pi}\left[\frac{1}{2}\cos\left(\frac{2A_x}{B_0L}\right) + \exp\left(\frac{2A_y}{B_0L}\right)\right] + P_0, \tag{8}$$

where P_0 is a uniform pressure of the background plasma. Harrison and Neukirch[23] found a distribution function $f_s^{hn}(H_s, p_{xs}, p_{ys})$ that allows one to obtain P_{zz} in form (8) directly from expression (3)

$$f_s^{hn} = n_{0s}\left(\frac{m_s\beta_s}{2\pi}\right)^{3/2} e^{-\beta_s H_s}[\exp(\beta_s u_{ys}p_{ys}) + a_s\cos(\beta_s u_{xs}p_{xs}) + b_s], \tag{9}$$

where u_{xs}, u_{ys}, a_s, b_s, and β_s are some positive constants. The first term in the distribution function f_s^{hn} has the same form as in the Harris model[22] and corresponds to the population responsible for the current density j_y. The second term describes the particle population carrying the current j_x and generating the magnetic field component B_y given by Eq. (5). The last term corresponds to the background plasma which does not contribute to the current. However, the

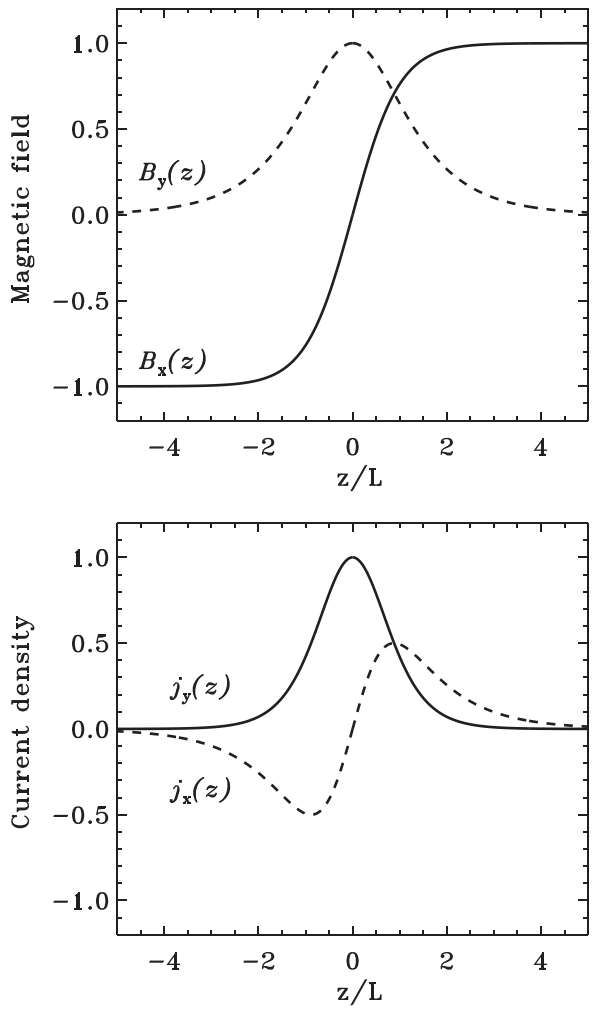

FIG. 1. Components of the magnetic field in a force-free Harris current sheet, given by Eqs. (4) and (5) (top panel), and the corresponding current densities (bottom panel). Both components of the magnetic field are normalised to the field amplitude B_0. Current components are normalised to their amplitude $cB_0/(4\pi L)$.

choice of the distribution function of form (9) results in uniform density and temperature profiles across the CS.[1,23] These conditions put strong restrictions on the solution from a physical point of view. In fact, it would be natural to expect that the plasma temperature and density are non-uniform across the CS, as the plasma may be hotter in the vicinity of regions of higher electric current due to heating, e.g., Ohmic heating or current-driven micro-turbulence. The need for a non-uniform distribution of the plasma temperature and density can also be connected with boundary conditions.

In order to obtain the equilibrium state of the force-free CS with inhomogeneous density and temperature profiles, the distribution function f_s^{hn} must be adjusted accordingly. Such a modification of f_s^{hn} can be achieved by introducing different temperatures for the two current-carrying populations. Namely, the parameter β_s in expression (9) characterises the temperature of both particle populations. Now, we introduce a more general distribution function assuming that the second current-carrying population is characterised by a temperature different by a positive factor of γ. The new distribution function f_s can be written in the following form:

$$f_s = n_{0s}\left(\frac{m_s\beta_s}{2\pi}\right)^{3/2}[e^{-\beta_s H_s}\exp(\beta_s u_{ys}p_{ys}) + a_s\gamma^{3/2}e^{-\gamma\beta_s H_s}\cos(\gamma\beta_s u_{xs}p_{xs}) + b_s\gamma^{3/2}e^{-\gamma\beta_s H_s}]. \quad (10)$$

The function f_s reduces to the function f_s^{hn} (see Eq. (9)) for $\gamma = 1$. Similar to the distribution function given by expression (9), the first term in f_s is identical to the Harris model,[22] whereas the second term corresponds to the second current-carrying population with a different temperature. Basically, the distribution function of the background plasma can be chosen arbitrarily, with only the positiveness of f_s required to be satisfied. We have assumed that the temperatures of the second current-carrying and background populations are the same. In this case, the condition $b_s > a_s$ ensures the positiveness of the function f_s over the entire phase space $(\mathbf{v}, \mathbf{r})$.

Substitution of distribution function (10) into Eq. (3) allows one to calculate a new pressure function P_{zz}

$$P_{zz}(A_x, A_y, \phi) = \sum_{s=i,e}\beta_s^{-1}n_{0s}G_s(A_x, A_y, \phi), \quad (11)$$

where

$$G_s = e^{-\beta_s q_s\phi}\exp(\beta_s q_s u_{ys}A_y)\exp(\beta_s m_s u_{ys}^2/2) + a_s\gamma^{-1}e^{-\gamma\beta_s q_s\phi}\exp(-\beta_s m_s\gamma u_{xs}^2/2)\cos(\gamma\beta_s u_{xs}q_s A_x) + b_s\gamma^{-1}e^{-\gamma\beta_s q_s\phi}.$$

The total electric charge density σ can be determined as a function of A_x and A_y by taking the derivative of the pressure P_{zz} given by Eq. (11), with respect to the electric potential ϕ (see Ref. 39)

$$\sigma = -\frac{\partial P_{zz}}{\partial\phi} = \sum_{s=i,e}q_s n_{0s}N_s(A_x, A_y, \phi), \quad (12)$$

where $n_{0s}N_s$ is the number density of the species s, and N_s is determined as

$$N_s = e^{-\beta_s q_s\phi}\exp(\beta_s q_s u_{ys}A_y)\exp(\beta_s m_s u_{ys}^2/2) + a_s e^{-\gamma\beta_s q_s\phi}\exp(-\beta_s m_s\gamma u_{xs}^2/2)\cos(\gamma\beta_s u_{xs}q_s A_x) + b_s e^{-\gamma\beta_s q_s\phi}.$$

Applying the quasi-neutrality condition $\sigma = 0$, satisfied by $N_i(A_x, A_y, \phi) = N_e(A_x, A_y, \phi)$, allows one to determine the transverse profile of the scalar potential ϕ. In the case, when ϕ does not vanish, our initial assumption that $P_{zz}(A_x, A_y)$ is an additive function $(P_{zz} = P_1(A_x) + P_2(A_y))$ cannot be satisfied. We focus on a particular class of models satisfying the exact neutrality condition, i.e., $\phi = 0$, imposing the following relations between the microscopic parameters of the ion and electron distribution functions:

$$n_{0e}\exp(\beta_e m_e u_{ye}^2/2) = n_{0i}\exp(\beta_i m_i u_{yi}^2/2) \equiv n_0,$$
$$a_e n_{0e}\exp(-\beta_e m_e\gamma u_{xe}^2) = a_i n_{0i}\exp(-\beta_i m_i\gamma u_{xi}^2) \equiv a,$$
$$b_e\exp(-\beta_e m_e u_{ye}^2/2) = b_i\exp(-\beta_i m_i u_{yi}^2/2) \equiv b,$$
$$-\beta_e u_{xe} = \beta_i u_{xi},$$
$$-\beta_e u_{ye} = \beta_i u_{yi}.$$

If one of these conditions is violated, the electrostatic field appears, and our approach becomes inapplicable. Taking these relations into account, we find that the pressure P_{zz} of the neutral plasma can be re-written in the following form:

$$P_{zz} = (\beta_e^{-1} + \beta_i^{-1}) n_0 [\exp(-e\beta_e u_{ye} A_y) + a\gamma^{-1}\cos(\gamma e\beta_e u_{xe} A_x) + b\gamma^{-1}]. \quad (13)$$

Direct comparison of (13) with (8) allows one to establish the following relations between the microscopic and macroscopic parameters:

$$\begin{aligned} B_0^2 &= 8\pi n_0(\beta_e^{-1} + \beta_i^{-1}), \\ a &= \gamma/2, \\ b &= 8\gamma\pi P_0/B_0^2, \\ L &= (2\pi n_0 e^2 u_{ye}^2 \beta_e^2 (\beta_i^{-1} + \beta_e^{-1}))^{-1/2}, \\ u_{ys} &= \gamma u_{xs}. \end{aligned}$$

In Eq. (12), the plasma density $n = n_{0i}N_i = n_{0e}N_e$ is determined as

$$n = n_0\{\exp(e\beta_i u_{yi} A_y) + a\cos(\gamma e\beta_i u_{xi} A_x) + b\}.$$

Using the explicit dependencies $A_{x,y}(z)$, given by Eqs. (6) and (7), we obtain the explicit expression for the plasma density $n(z)$

$$n(z) = n_0\left(\frac{\gamma}{2} + b\right) + n_0(1-\gamma)\cosh^{-2}(z/L). \quad (14)$$

We note that the plasma density can also be written as $n = n_1 + n_2$, where $n_1 = n_0\cosh^{-2}(z/L)$ is the density of the first current carrying population, while $n_2 = n_0 b + n_0\gamma(1/2 - \cosh^{-2}(z/L))$ is the combined density of the second current-carrying population and background population. The density of the first population peaks in the central region of the CS, while the total density of other populations has a minimum there. We recall that these separate populations still correspond to the same plasma species. Substitution of (6) and (7) into (13) allows one to calculate the explicit value of the pressure P_{zz}, which is uniform according to the force-free condition

$$P_{zz} = n_0\gamma^{-1}\left(\beta_e^{-1} + \beta_i^{-1}\right)\left(\frac{\gamma}{2} + b\right). \quad (15)$$

Eq. (15) together with (14) gives us the variation of the plasma temperature $T = P_{zz}/n(z)$ across the CS

$$T(z) = \frac{\gamma^{-1}\left(\beta_i^{-1} + \beta_e^{-1}\right)\cosh^2(z/L)}{2(1-\gamma)/(\gamma + 2b) + \cosh^2(z/L)}. \quad (16)$$

We can clearly see that the plasma temperature and density profiles are uniform ($n = n_0(1/2 + b)$ and $T = \beta_i^{-1} + \beta_e^{-1}$) only in the case $\gamma = 1$, in accord with the original Harrison and Neukirch[23] model. In the case, when the temperatures of the current-carrying populations are different, i.e., $\gamma \neq 1$, the plasma temperature and density profiles become non-uniform. We note that $\gamma > 1$ ($\gamma < 1$) describes a CS with the first current-carrying population hotter (colder) than the second population. The density and temperature profiles normalised to their values at the CS boundary $n_0(\gamma/2 + b)$ and $\gamma^{-1}(\beta_e^{-1} + \beta_i^{-1})$, respectively, are illustrated in Figs. 2 and 3. To keep the distribution function given by Eq. (10) positive, the density of the background population should be set appropriately. The condition $b > a = \gamma/2$ ensures that the distribution function is positive over the entire phase space ($\mathbf{v}$, $\mathbf{r}$).

In Fig. 2, the parameter b is fixed ($b = 10$) and the density and temperature profiles are illustrated for various values of the parameter γ ($\gamma < 2b$). For $\gamma > 1$, the temperature peaks at the CS central region, while the density is depleted so that the plasma pressure P_{zz} is uniform (as it should be for a force-free CS). Larger values of the parameter γ result in a stronger plasma density depletion in the CS central region. We note that in the limiting case $\gamma \gg 1$ and $b \approx \gamma/2$ (not illustrated in Fig. 2, where the parameter b is fixed), the plasma density in the central region of the CS asymptotically tends to a small value. The temperature peak in the CS

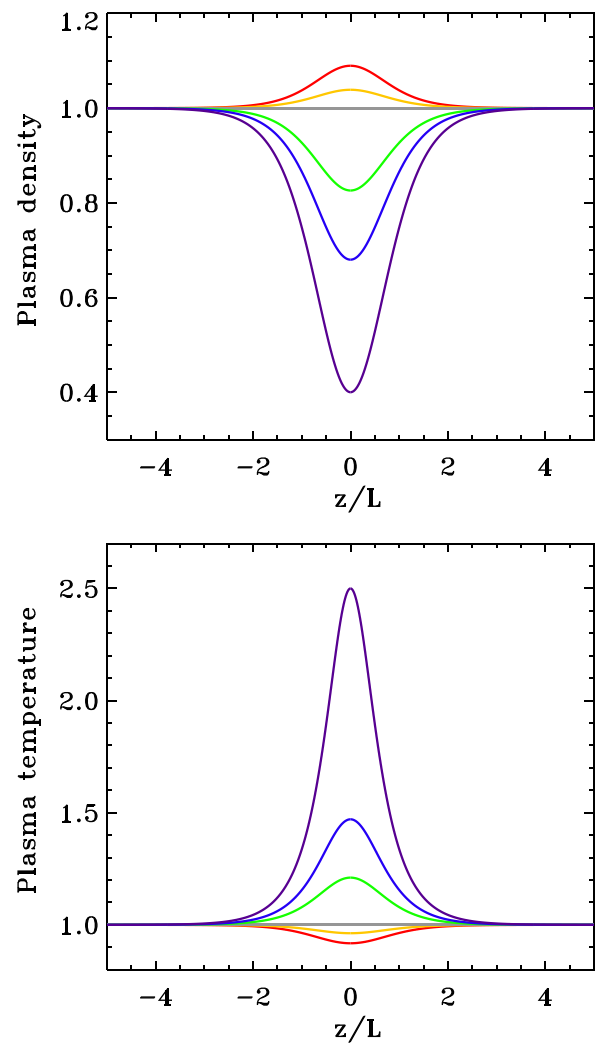

FIG. 2. Density and temperature profiles across a current sheet, determined by Eqs. (14) and (16), plotted for $b = 10$ and $\gamma = 0.1$ (red lines), $\gamma = 0.6$ (orange lines), $\gamma = 1$ (grey lines), $\gamma = 3$ (green lines), $\gamma = 5$ (blue lines), and $\gamma = 10$ (purple lines). The plasma density profile is normalised to $n_0(\gamma/2 + b)$; the temperature profile is normalised to $(\beta_i + \beta_e)/\gamma\beta_i\beta_e$.

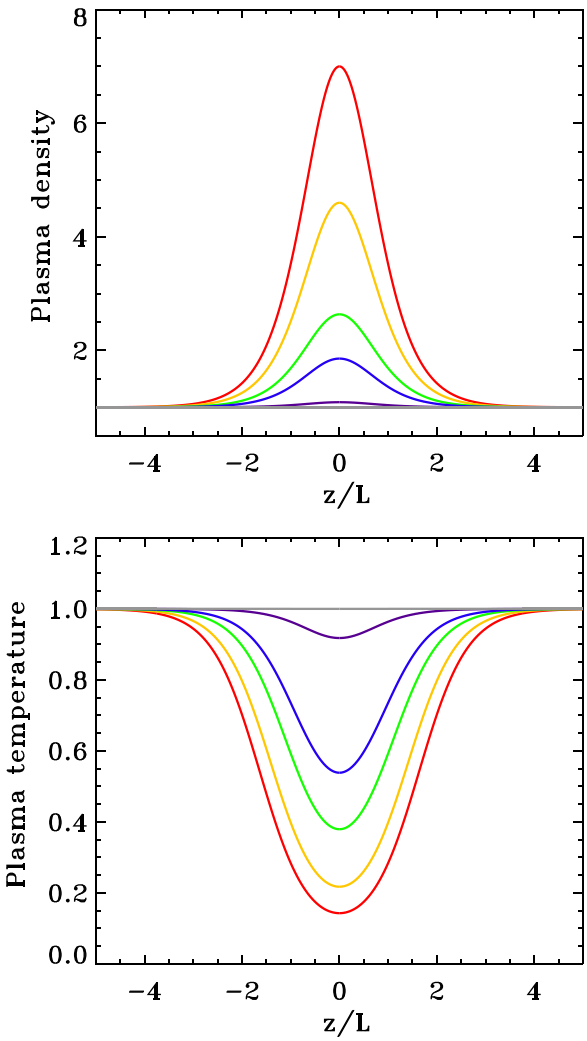

FIG. 3. Density and temperature profiles across a current sheet, determined by Eqs. (14) and (16), plotted for $\gamma = 0.1$ and for various values of the background plasma density: $b = 0.1$ (red lines), $b = 0.2$ (orange lines), $b = 0.5$ (green lines), $b = 1$ (blue lines), and $b = 10$ (purple lines). The limit $b \gg 1$ is shown by the horizontal grey lines. The plasma density profile is normalised to $n_0(\gamma/2 + b)$; the temperature profile is normalised to $(\beta_i + \beta_e)/\gamma\beta_i\beta_e$.

central region forms due to the first current-carrying population which is hotter than the second population (in the case $\gamma > 1$) and localised near the CS central region (as $n_1 = n_0 \cosh^{-2}(z/L)$). The density of the second, colder, current-carrying population increases toward the CS boundary resulting in the plasma temperature decrease.

For $\gamma < 1$, the first current-carrying population is colder than the second population. In contrast to the previous case, Fig. 2 shows that the plasma temperature has a minimum in the CS central region, while the plasma density peaks therein. The density peak is larger for smaller values of γ. In the limiting case $\gamma \approx 0$, the density variation across the CS is less than 10% of the plasma density at the CS boundary. Eq. (14) shows that for $\gamma \approx 0$ the plasma density in dimensionless units is $n(z) = 1 + b^{-1}\cosh^{-2}(z/L)$, so that the 10% density variation corresponds to $b = 10$, i.e., to the assumed density of the background population.

In Fig. 3, we fix the temperature ratio to a small value, $\gamma = 0.1$, implying the second current-carrying population to be ten times hotter than the first one. We vary the density of the background population b, satisfying the condition $b > \gamma/2$ to ensure the positiveness of the distribution functions. Smaller values of the background population density are found to result in a larger variation of the plasma density across the CS. In particular, for $b = 0.1$, the plasma density (temperature) in the CS central region is ten times larger (smaller) than at the CS boundary. In the limit $b \gg 1$, the plasma density and temperature become approximately uniform across CS.

III. DISCUSSION AND CONCLUSIONS

We have generalised the models developed in Refs. 23 and 33 taking into account the density and temperature variations across the CS that can arise in realistic natural and laboratory plasma systems either due to the boundary conditions or Ohmic heating in the region of the enhanced current density localisation. The latter process should be slow enough to consider the developed models as quasi-stationary. One of the motivations for our work was a shortcoming of the model developed by Harrison and Neukirch,[23] which only provides uniform density and temperature profiles and does not inform whether the inhomogeneous profiles of the plasma parameters consistent with MHD solutions are possible. In fact, it is clear that as the CS thickness becomes larger than characteristic kinetic scales, it should be possible to set arbitrary density and temperature profiles across the CS, while maintaining a constant plasma pressure. The kinetic models designed here show that the density and temperature profiles can actually be set arbitrarily not only in the MHD limit, i.e., in the case when the CS thickness is much larger than kinetic scales, but also in the kinetic regime.

In the developed models, the density and temperature may either increase or decrease in the CS central region. Such configurations can be found in a number of astrophysical and space plasma systems, in particular, in solar coronal streamers and in macroscopic CSs over the reconnection sites in solar flares. The force-free CS models with the plasma density peaked in the CS central region, developed here, represent effective waveguides for MHD waves. Specifically, regions of decreased Alfvén speed are fast magnetoacoustic waveguides. Currently, coronal MHD seismology studies assume that CSs are described by the Harris model,[26,30,43] where the plasma β is infinite in the CS central region (where the magnetic field vanishes) and drops to some small values at the CS boundary. In the developed force-free models, the plasma β is always constant across CS and is given by $\beta = 8\pi P_{zz}/B_0^2 = 1/2 + b/\gamma$ (according to Eq. (15) and using the relation $B_0^2 = 8\pi n_0(\beta_i^{-1} + \beta_e^{-1})$). Taking into account that $b > \gamma/2$ to ensure the positiveness of the particle distribution functions, we find that in the developed force-free CSs the parameter $\beta > 1$. Thus, the properties of MHD waves in such a CS should be different from those in the Harris model.[26,30] The properties of MHD waves in such a force-free configuration are worth considering and may be used for MHD seismology purposes.[14,32] Additionally, kinetic models of the developed force-free CSs generalised for relativistic plasmas[44] could be useful for modelling CS instabilities in pulsar winds.[21]

Recently, there have been reports of *in situ* observations of force-free CSs in the magnetotails of Jupiter[4] and the Earth.[3,46] Similar force-free CSs are studied in detail in laboratory plasmas.[15] The principal feature of these force-free CSs is the presence of a finite magnetic field component B_z. Models have been developed for almost force-free CSs including an asymptotically small[2] and finite[46] B_z component. It has been shown both theoretically[46] and observationally[4,46] that the plasma density is uniform in these CSs. In force-free CSs with a finite B_z, the density and temperature profiles cannot be set arbitrarily even in the MHD limit, since the field lines are curved and cross the entire CS. In contrast, the magnetic field lines are straight for the models developed in the present paper (i.e., each field line is "tied" to a particular z coordinate). The plasma parameters can therefore be set arbitrarily for each field line satisfying the condition of total pressure balance. Thus, the force-free CS models developed in the present paper can be applied only to situations without a regular B_z component.

ACKNOWLEDGMENTS

The authors acknowledge the support by the British Council Researcher Links Programme. The work of I.V. was supported by the Russian foundation for Basic Research (RFBR) Grant No. 13-02-00454. The work of V.N. was supported by STFC consolidated Grant No. ST/L000733/1. The authors are grateful to Dr. David Pascoe for discussions.

[1]B. Abraham-Shrauner, Phys. Plasmas **20**(10), 102117 (2013).
[2]A. V. Artemyev, Phys. Plasmas **18**(2), 022104 (2011).
[3]A. V. Artemyev, A. A. Petrukovich, A. G. Frank, R. Nakamura, and L. M. Zelenyi, J. Geophys. Res. **118**, 2789–2799, doi:10.1002/jgra.50297 (2013).
[4]A. V. Artemyev, I. Y. Vasko, and S. Kasahara, Plan. Sp. Sci. **96**, 133–145 (2014).
[5]M. Balikhin and M. Gedalin, J. Plasma Phys. **74**, 749 (2008).
[6]V. S. Beskin, S. V. Chernov, C. R. Gwinn, and A. A. Tchekhovskoy, Space Sci. Rev. **191**, 207 (2015).
[7]J. Birn, M. F. Thomsen, and M. Hesse, Phys. Plasmas **11**, 1825–1833 (2004).
[8]D. Biskamp, *Nonlinear Magnetohydrodynamics* (Cambridge University Press, Cambridge, UK, 1997).
[9]E. Camporeale and G. Lapenta, J. Geophys. Res. **110**, A07206, doi:10.1029/2004JA010779 (2005).
[10]F. Catapano, A. V. Artemyev, G. Zimbardo, and I. Y. Vasko, Phys. Plasmas **22**(9), 092905 (2015).
[11]F. Ceccherini, C. Montagna, F. Pegoraro, and G. Cicogna, Phys. Plasmas **12**(5), 052506 (2005).
[12]P. J. Channell, Phys. Fluids **19**, 1541–1545 (1976).
[13]I. De Moortel and P. Browning, Philos. Trans. R. Soc. London, Ser. A **373**, 40269 (2015).
[14]I. De Moortel and V. M. Nakariakov, Philos. Trans. R. Soc. London, Ser. A **370**, 3193–3216 (2012).
[15]A. Frank, S. Bugrov, and V. Markov, Phys. Lett. A **373**, 1460–1464 (2009).
[16]G. Fruit, P. Louarn, A. Tur, and D. Le Quéau, J. Geophys. Res. **107**, 1411, doi:10.1029/2001JA009212 (2002).
[17]G. Fruit, P. Louarn, A. Tur, and D. Le QuéAu, J. Geophys. Res. **107**, 1412, doi:10.1029/2001JA009215 (2002).
[18]W.-Z. Fu and L.-N. Hau, Phys. Plasmas **12**(7), 070701 (2005).
[19]V. Génot, F. Mottez, G. Fruit, P. Louarn, J. Sauvaud, and A. Balogh, Planet. Space Sci. **53**, 229–235 (2005).
[20]J. T. Gosling, Space Sci. Rev. **172**, 187–200 (2012).
[21]F. Guo, H. Li, W. Daughton, and Y.-H. Liu, Phys. Rev. Lett. **113**(15), 155005 (2014).
[22]E. Harris, Nuovo Cimento **23**, 115–123 (1962).
[23]M. G. Harrison and T. Neukirch, Phys. Rev. Lett. **102**(13), 135003 (2009).
[24]M. G. Harrison and T. Neukirch, Phys. Plasmas **16**(2), 022106 (2009).
[25]C. M. Jackman, C. S. Arridge, N. André, F. Bagenal, J. Birn, M. P. Freeman, X. Jia, A. Kidder, S. E. Milan, A. Radioti, J. A. Slavin, M. F. Vogt, M. Volwerk, and A. P. Walsh, Space Sci. Rev. **182**, 85–154 (2014).
[26]P. Jelínek and M. Karlický, Astron. Astrophys. **537**, A46 (2012).
[27]J. R. Kan, J. Geophys. Res. **78**, 3773–3781, doi:10.1029/JA078i019p03773 (1973).
[28]V. V. Kocharovsky, V. V. Kocharovsky, and V. J. Martyanov, Phys. Rev. Lett. **104**(21), 215002 (2010).
[29]K.-W. Lee and L.-N. Hau, J. Geophys. Res. **113**, A12209, doi:10.1029/2008JA013459 (2008).
[30]H. Mészárosová, M. Karlický, P. Jelínek, and J. Rybák, Astrophys. J. **788**, 44 (2014).
[31]I. Mochol and J. Pétri, Mon. Not. R. Astron. Soc. **449**, L51–L55 (2015).
[32]V. M. Nakariakov and L. Ofman, Astron. Astrophysics **372**, L53–L56 (2001).
[33]T. Neukirch, F. Wilson, and M. G. Harrison, Phys. Plasmas **16**(12), 122102 (2009).
[34]E. V. Panov, A. V. Artemyev, R. Nakamura, and W. Baumjohann, J. Geophys. Res. **116**, A12204, doi:10.1029/2011JA016860 (2011).
[35]E. N. Parker, *Spontaneous Current Sheets in Magnetic Fields: With Applications to Stellar X-Rays*, International Series in Astronomy and Astrophysics Vol. 1 (Oxford University Press, New York, 1994).
[36]A. Petrukovich, A. Artemyev, I. Vasko, R. Nakamura, and L. Zelenyi, Space Sci. Rev. **188**, 311–337 (2015).
[37]*Magnetic Reconnection: MHD Theory and Applications*, edited by E. Priest and T. Forbes (Cambridge University Press, Cambridge, UK, 2000).
[38]M. Roth, J. de Keyser, and M. M. Kuznetsova, Space Sci. Rev. **76**, 251–317 (1996).
[39]K. Schindler, *Physics of Space Plasma Activity* (Cambridge University Press, 2006).
[40]K. Schindler and J. Birn, J. Geophys. Res. **107**, 1193, doi:10.1029/2001JA000304 (2002).
[41]M. I. Sitnov, M. Swisdak, P. N. Guzdar, and A. Runov, J. Geophys. Res. **111**, A08204, doi:10.1029/2005JA011517 (2006).
[42]M. I. Sitnov, L. M. Zelenyi, H. V. Malova, and A. S. Sharma, J. Geophys. Res. **105**, 13029–13044, doi:10.1029/1999JA000431 (2000).
[43]J. M. Smith, B. Roberts, and R. Oliver, Astron. Astrophys. **327**, 377–387 (1997), see http://adsabs.harvard.edu/abs/1997A%26A...327..377S.
[44]C. R. Stark and T. Neukirch, Phys. Plasmas **19**(1), 012115 (2012).
[45]R. A. Treumann and W. Baumjohann, Front. Phys. **1**, 31 (2013).
[46]I. Y. Vasko, A. V. Artemyev, A. A. Petrukovich, and H. V. Malova, Ann. Geophys. **32**, 1349–1360 (2014).
[47]I. Y. Vasko, A. V. Artemyev, V. Y. Popov, and H. V. Malova, Phys. Plasmas **20**(2), 022110 (2013).
[48]F. Wilson and T. Neukirch, Phys. Plasmas **18**(8), 082108 (2011).
[49]M. Yamada, R. Kulsrud, and H. Ji, Rev. Mod. Phys. **82**, 603–664 (2010).
[50]P. H. Yoon, M. S. Janaki, and B. Dasgupta, J. Geophys. Res. **119**, 260–267, doi:10.1002/2013JA019617 (2014).
[51]P. H. Yoon and A. T. Y. Lui, J. Geophys. Res. **109**, A11213, doi:10.1029/2004JA010555 (2004).
[52]P. H. Yoon and A. T. Y. Lui, J. Geophys. Res. **110**, A01202, doi:10.1029/2003JA010308 (2005).
[53]L. Zelenyi and A. Artemyev Space Sci. Rev. **178**, 441–457 (2013).
[54]L. M. Zelenyi and V. V. Krasnoselskikh, Sov. Astron. **23**, 460 (1979), see http://adsabs.harvard.edu/abs/1979SvA....23..460Z.
[55]L. M. Zelenyi, H. V. Malova, A. V. Artemyev, V. Y. Popov, and A. A. Petrukovich, Plasma Phys. Rep. **37**, 118–160 (2011).